Research Article

Nano Biomed Eng

Fabrication, Characterization, and *In Vitro* Testing of Quercetin–Copper(II) Complex

Sidra Sajid[1,§], Nazish Jahan[1,§], Zille Huma[2], Muhammad Ishaq Ali[3], Amir Zada[3], Aliya Ibrar[4], Ghulam Abbas Ashraf[5], Laila Noureen[6], Muhammad Ayaz[7], Samia Arain[8] ✉, Faiq Saeed[9] ✉

[1] Department of Chemistry, University of Agriculture, Faisalabad, Pakistan
[2] Department of Chemistry, Riphah International University, Faisalabad, Pakistan
[3] Department of Chemistry, Abdul Wali Khan University Mardan, Khyber Paktunkhwa, Pakistan
[4] Department of Chemistry, University of Haripur, Pakistan
[5] New Uzbekistan University, Tashkent 100007, Uzbekistan
[6] MTA-SZTE Momentum, Biocollids Research Group, Department of Physical Chemistry and Materials Science, University of Szeged, Szeged H-6720, Hungary
[7] School of chemical Engineering and Technology, Tianjin University, Tianjin 300072, China
[8] Tianjin Key Laboratory of Low Dimensional Materials Physics and Preparing Technology, School of Science, Tianjin University, Tianjin 300072, China
[9] Tianjin Key Laboratory of Molecular Optoelectronic Science, Department of Chemistry, School of Science, Tianjin University, Tianjin 300072, China

[§] These authors contributed equally to this work.

✉ Corresponding authors. Samia Arain, samia.arain100@gmail.com; Faiq Saeed, faiqsaeed@tju.edu.cn

Received: Jan. 28, 2024; **Revised:** Mar. 16, 2024; **Accepted:** Apr. 15, 2024

Citation: S. Sajid, N. Jahan, Z. Huma, et al. Fabrication, characterization, and *in vitro* testing of quercetin–copper(ii) complex. *Nano Biomedicine and Engineering*, 2024, 16(3): 402–415.

http://doi.org/10.26599/NBE.2024.9290085

Abstract

Quercetin is a biologically active and widely used dietary flavonoid with robust antioxidant and chelating effects. However, due to its lesser solubility, it has poor bioavailability, which results in limited medicinal effects. This study synthesized quercetin–metal complexes, which enhanced the medicinal properties and bioavailability of quercetin. Quercetin–copper (Cu) complexes were fabricated by using copper sulfate and copper chloride in the Quercetin/Cu ratios of 1:2 and 1:1, respectively. Furthermore, Cu complexes with quercetin extracted from onion peels or standard quercetin were obtained. The current research also sought to assess the bioavailability as well as antibacterial and antioxidant properties. Spectrophotometry revealed that better complexes were prepared with a ratio of 1:2 as compared to 1:1. Copper chloride and copper sulfate showed no significant ($p < 0.05$) effects on complex formation. These metal complexes had a considerable impact on *Bacillus subtilis* (Gram$^+$) as compared to *Escherichia coli* (Gram$^-$). The pharmacokinetic parameters indicated that the oral bioavailability of quercetin–Cu(II) complexes was significantly enhanced as compared to pure quercetin. The results of this study suggested the successful formation of quercetin–metal complexes, which markedly increased the bio-availability of quercetin.

Keywords: quercetin; quercetin–Cu(II) complex; spectroscopic analysis; antioxidant and antimicrobial assays; pharmacokinetic studies

Introduction

A class of naturally occurring bioactive polyphenols known as flavonoids has potent antioxidant effects [1]. They are abundant in the environment and mostly originate from nourishments consumed by humans, i.e., fruits, veggies, and grains, as well as beverages like beer, cider, and tea [2, 3]. They are benzopyrone derivatives with a flavylium cation-based primary structure [4]. The chemical structure of a flavonoid, which governs its activity, is intimately correlated with the quantity of hydroxyl (OH) groups present [5–7]. In general, more free OH groups correlate with more robust antioxidant activity [8]. Flavonoids continue to demonstrate a number of positive benefits on human health, including anticarcinogenic, antitumor [9], antiplatelet, antiallergic, virucidal, bacteriostatic [10], vasodilatory [5], and reactive oxygen species (ROS) and radical quenching activities.

The common dietary flavonoid quercetin holds medicinal promise for treating a number of health issues, like asthma, cancer [11], Alzheimer's disease, coronary artery disease, pancreatitis [12], and prostatitis. However, due to relatively low permeability, poor bioavailability [13], negligible solubility, and instability, its therapeutic properties are constrained. The inadequate bioavailability has prompted efforts to boost ingestion. Through chelation with metallic ions, quercetin can create complexes that remain stable [14] and enhance the superoxide dismutase (SOD) activity by initiating the coordinating metallic composition [15]. Inhibiting free radical production may require the metal chelation technique, which leads to the destruction of the targeted biomolecules [16].

Metal–quercetin complexes serve a crucial function in the biological process and have a greater bioavailability. Their significant contributions have resulted in the reduction of heavy metal toxicity [17] and the biological utilization of metals. They can also impede lipid peroxidation [18]. Moreover, they are natural metal chelators and can inhibit Fenton reactions. Furthermore, compared to the free form, the antioxidant capabilities of quercetin were improved when complexed with copper. Quercetin–copper (Cu) complexes exhibit a more potent antioxidant effect [19], tumor-inhibiting properties, lower swelling [20], fight antipathies [21], and shield cutaneous tissues [22]. Therefore, ongoing research on quercetin–metal complexes is crucial for the creation of novel medications and for devising cutting-edge approaches for drug screening [23, 24].

In the current experiment, quercetin–Cu complexes were fabricated utilizing a variety of salt types and ratios. Then, their antioxidant and antibacterial capabilities were also assessed. Ultraviolet–visible (UV–Vis) spectroscopy and Fourier Transform Infrared (FTIR) spectroscopy were used for their characterization. Furthermore, this study examined the chemical mechanisms of the bioavailability of the complexes in rats.

Materials and Methodology

Synthesis of complexes

The complexes were synthesized using standard quercetin or that extracted from onion (*Allium cepa*) peels [25], as shown in Fig. 1.

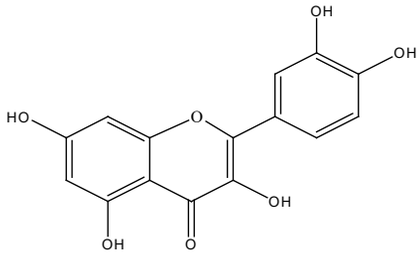

Fig. 1 The primary chemical structure of quercetin.

Collection of raw material

Onion skins were obtained from a nearby store. Before extraction, the skin was cleaned, powdered into a finely ground form, and stored in a sealed, airtight container [26].

Quercitin extraction

A Soxhlet device was used for the extraction. First, 40 g of powdered onion peel was placed in a cellulose thimble, and 400 mL of methanol was added. Then, the complete equipment was placed in a water bath. The six-hour extraction process continued till the solvent began to boil. The liquid extract was filtered utilizing a Whatman filter paper and condensed using a rotary evaporator. The concentrates were stored in a refrigerator [27, 28].

Standard material

Standard material is that with a known concentration. In this study, extracted quercetin was used as the standard material [29].

Fabrication of quercetin–Cu(II) complexes

Copper chloride and copper sulfate in two distinct weight ratios (Quer–Cu = 1:1 and 1:2) were used to prepare the quercetin–Cu(II) complexes [30, 31].

Fabrication of complexes with sulfate salt

A container with a spherical bottom, an electric stirrer, and a thermometer were used to prepare the complexes. Briefly, 20 mL of methanol and 0.01 mol of solid quercetin were mixed in the flask, and the mixture was stirred until the solution changed from colorless to brilliant yellow. The color of the reaction mixture changed to dark yellow with continuous agitation for 2 h at room temperature after adding solid copper (0.02 mol $CuSO_4 \cdot 5H_2O$) to the mixture. The mixture was subsequently cleaned, evaporated at ambient temperature, and washed with ter-butanol to get rid of the uninspiring part of the reagent. This product was air-dried at room temperature for a day [32].

Fabrication of complexes with chloride salt

The reaction chamber of the flask was filled with 0.01 mol quercetin and 20 mL of MeOH, which was then agitated until the solid quercetin dissolved entirely. The solution went from being colorless to pale yellow. Following the addition of 0.02 mol $CuCl_2 \cdot 2H_2O$ to the flask, the color changed to a brownish yellow. The pH was adjusted to 10 with NaOH. After 2 h of stirring and washing with 3:1 methanol–water, the uninventive component of the reagent was removed by filtering off the brownish yellow precipitate. The product was air-dried for three days at room temperature [33].

Types of quercetin–Cu(II) complexes

In total, eight quercetin–Cu(II) complexes were obtained. The metal complexes i, ii, iii, and iv were synthesized using pure standard quercetin with $CuSO_4$ or $CuCl_2$ in the ratios of 1:2 and 1:1, respectively. The metal complexes v, vi, vii, and viii were synthesized using the quercetin extracted from onion peels with $CuSO_4$ or $CuCl_2$ in the ratios of 1:2 and 1:1, respectively.

Characterization of the complexes

Standard quercetin and its compounds were examined using UV–Vis spectroscopy (PerkinElmer, USA) and 1 cm quartz cells [34, 35]. For this, 10 mL of quercetin or the quercetin–Cu complex was dissolved in 10 mL of methanol to produce a 1 000 μg/mL solution. The spectrum, between 200 and 800 nm, was captured [36]. The FTIR spectra were obtained using a KBr matrix pellet and an IR spectrometer (Perkin Elmer, USA) in the spectral range of 400–4 000 cm^{-1} [37, 38].

Antioxidant potential

The stable 2,2-diphenyl-1-picrylhydrazyl (DPPH) radical and linoleic acid tests were employed to measure the antioxidant activity.

DPPH scavenging assay

The capacity of quercetin–metal complexes to scavenge free radicals was tested by employing the following procedure. Standard quercetin and quercetin–Cu complexes were produced at five different levels at 20–100 g/mL. Next, 3 mL of each level was added to the 0.1 mmol/L DPPH stock solution and incubated in the dark for 30 min. The OD_{517} was measured on a UV–Vis spectrophotometer. DPPH solution was used as a blank to quantify DPPH decay. The inhibition of the DPPH radical (%) was determined using the following equation:

$$\text{DPPH inhibition (\%)} = (1 - A_1/A_0) \times 100$$

where A_1 is the absorbance of the sample, and A_0 is the absorbance of the control.

Reducing power assay

The reducing power of quercetin–metal complexes was calculated using the following method. First, five different concentrations of standard quercetin and quercetin–Cu complexes (20–100 g/mL) were prepared. Then, 2.5 mL of 1% potassium ferricyanide and 2.5 mL of 0.2 mol/L phosphate buffer (pH 6.6) were added to each reaction mixture. They were then incubated at 50 °C for 20 min. Next, 2.5 mL of 1% trichloroacetic acid was added, and the mixture was centrifuged at 3 000 r/min. Finally, the topmost layer was removed; 2 mL of it was added with 0.5 mL of 0.1% ferric chloride (v/v) and 25 mL of distilled water and mixed. The OD_{700} was measured using a spectrophotometer [39]. The control sample contained all these reagents except the complexes.

Antioxidant activity in the linoleic acid system

Briefly, 2 mL of 0.04 mol/L phosphate buffer (pH 7) and 2.5 mL of a linoleic acid emulsion were mixed with 500 μg of the quercetin–Cu complex. This reaction mixture was incubated at 37 °C for 72 h to facilitate rapid oxidation. After 24 h, 2 mL of this

mixture was collected and blended with 0.5 mL of 30% ammonium thiocyanate, 0.5 mL of $FeCl_2$, and 0.5 mL of 0.02 mol/L $FeCl_2$. Then the OD_{500} was measured. Pure quercetin served as the control. The samples were analyzed each day [40]. The inhibition of lipid peroxidation (%) was calculated as follows:

$$\text{Inhibition of lipid peroxidation (\%)} = 100 - (A_1/A_0) \times 100$$

where $A_1$is the absorbance of the sample and A_0 is the absorbance of the control.

Anti-microbial activity

The antibacterial effects of quercetin (Quer) and the synthesized quercetin–Cu(II) complexes were assessed using the well-diffusion method [41]. *Bacillus subtilis* ($Gram^+$) and *Escherichia coli* ($Gram^-$) were the two bacterial species tested for antibacterial activity. Nutrient agar was prepared in distilled water and pH was adjusted to 7. The bacterial culture was dispersed across the agar plates using a clean cotton bud and was maintained for 24 h at 37 °C in an incubator. Sterile media was placed on Petri plates, and they were left to build up. These poured plates were incubated in a 37 °C oven. Clean plates were chosen for further processing after 24 h. Standard quercetin, metal complexes, and ciprofloxacin solutions of 20, 40, 60, 80, and 100 μg/mL were prepared by dissolving them in 1 mL of water. Ciprofloxacin was used as an additive to contrast the activities of the samples. Next, 6-mm wells were formed in the Petri plates containing killed bacteria. After placing samples in the wells, the plates were incubated for 24 h at 37 °C. In the end, the zone of inhibition (mm) was measured using a zone reader [42].

Pharmacokinetic studies

Male rats weighing 250–300 g were chosen to study the pharmacokinetics of the quercetin-copper complexes. All the procedures and handlings were approved by the Ethical Committee of the Riphah International University (No. CE/1429 Dated 07-07-2022). The rats were randomly distributed into three groups of three rats each, totaling nine rats (Table 1). Of these, one group was selected as the control, the second received quercetin orally, and the third received a quercetin-copper complex at 50 mg/kg. From the abdominal aorta of each rat, 1 mL of blood was drawn at predetermined time points of 0.5, 1, 2, 4, 6, and 24 h and placed into lithium heparin tubes. The plasma was extracted from the blood, centrifuged, and stored at −20 °C [43–45].

The procedure used to extract quercetin and quercetin-copper complexes from plasma samples was as follows. Briefly, 400 μL of methanol and 200 μL of 25% HCl were added to 200 μL of plasma. This reaction mixture was vortexed for 30 s, centrifuged, and incubated at 50 °C for 15 min in a water bath. A 20 μL of the upper layer was subjected to HPLC to determine the plasma levels of quercetin. Methanol, acetonitrile, and 30 mmol/L NaH_2PO_4 were mixed in a ratio of 65:29:6 (v/v/v) to form the mobile phase. A C18 column was utilized. Elution was carried out in gradient mode at a flow rate of 1 mL/min; a UV-detector set to 370 nm was used [46].

Statistical tools

The data was analyzed using a one-way analysis of variance (ANOVA) and Tukey's test [47].

Results and Discussion

Synthesis of quercetin–Cu(II) complexes

Quercetin–Cu(II) complexes synthesized using copper sulfate were dark yellow, and those prepared using copper chloride were brownish yellow. The change in the solution color indicated the formation of metal complexes.

Physical properties of the metal complexes

The yellow complexes were stable at room temperature. Complexes were insoluble in water but only marginally in chloroform. All were soluble in ethanol, methanol, dimethyl sulfoxide (DMSO), and dimethylformamide (DMF).

UV–Vis spectroscopy

The UV–Vis absorption spectra of standard quercetin, standard quercetin–Cu(II) complexes (metal

Table 1 The pharmacokinetic study

Sample No.	Groups	Dose (mg/kg)
1	Control group (n = 3)	—
2	Quercetin administered group (n = 3)	50
3	Quercetin-copper complex administered group (n = 3)	50

complexes i, ii, iii, and iv), and extracted quercetin–Cu(II) complexes (metal complexes v, vi, vii, and viii) were recorded using methanol as a solvent at a range of 200–800 nm. Fig. 2 displays the

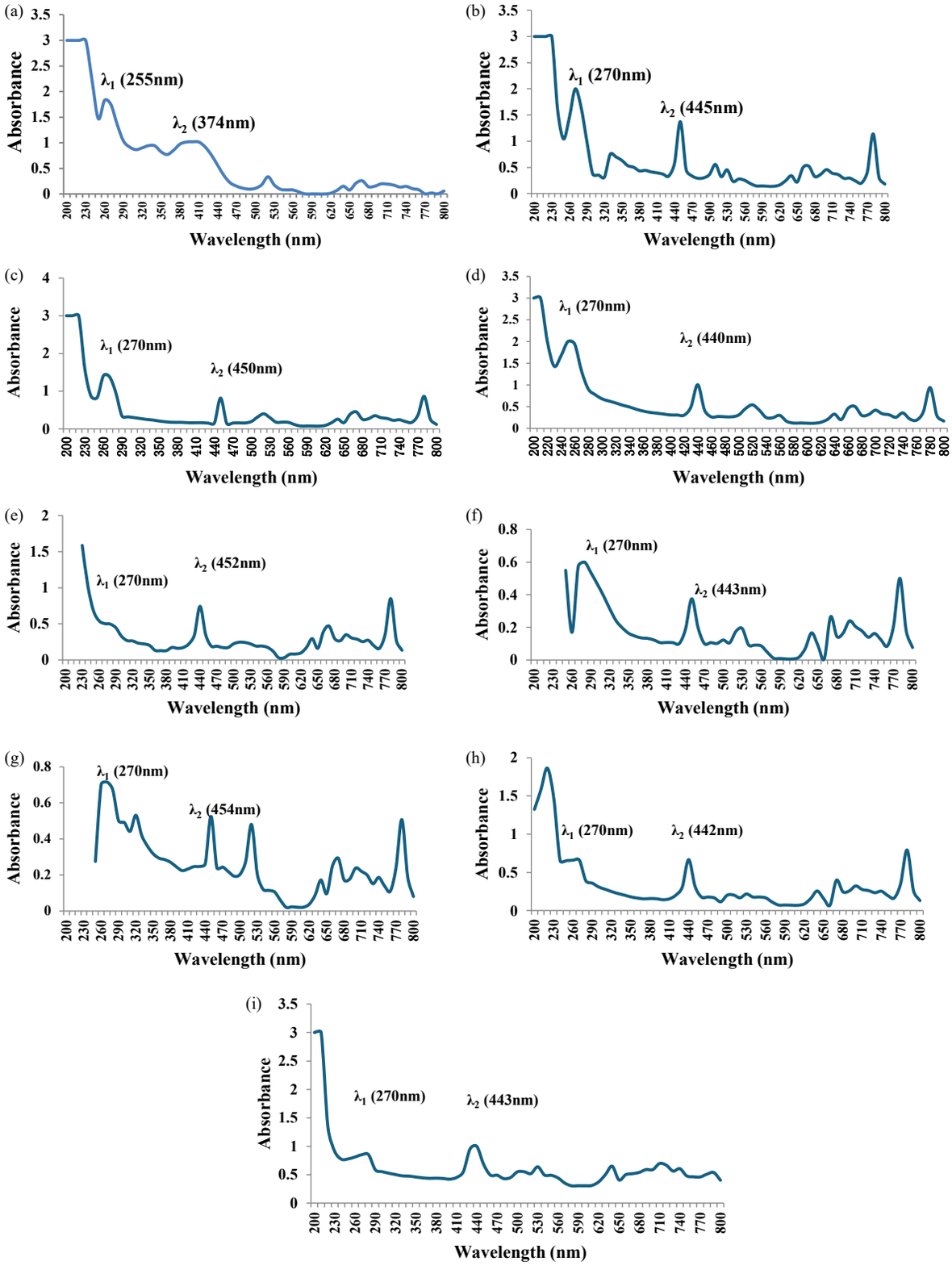

Fig. 2 UV–Vis spectra of quercetin and quercetin–Cu(II) complexes **(a)** quercetin, **(b)** metal complex-i (Quer with $CuSO_4$, ratio 1:2), **(c)** metal complex-ii (Quer with $CuSO_4$, ratio 1:1), **(d)** metal complex-iii (Quer with $CuCl_2$, ratio 1:2), **(e)** metal complex-iv (Quer with $CuCl_2$, ratio 1:1), **(f)** metal complex-v (extracted Quer with $CuSO_4$, ratio 1:2), **(g)** metal complex-vi (extracted Quer with $CuCl_2$, ratio 1:2), **(h)** metal complex-vii (extracted Quer with $CuSO_4$, ratio 1:2), and **(i)** metal complex-viii (extracted Quer with $CuCl_2$, ratio 1:1).

UV–Vis spectra of quercetin and quercetin–Cu(II) complexes. Due to the A ring absorption (benzoyl system) and B ring absorption (cinnamoyl system) of the quercetin molecule, two distinct absorption bands were observed at 255 nm (1) and 374 nm (2), respectively. The characteristic bands of the cinnamoyl system (2) in the spectra of the metal complexes i, ii, iii, iv,v, vi, vii, and viii were displaced from 374 to 445, 450, 440, 452, 443, 454, 442, and 443 nm, respectively. A hypochromic shift of the benzoyl system (1) from 255 to 270 nm was seen in the spectra of all the metal complexes. The development of quercetin–Cu(II) complexes was confirmed by the presence of bands of different wavelengths in the complexes and quercetin.

FTIR spectroscopy

The FTIR spectra confirmed the coordination between metal atoms and quercetin. The major bands with assignments are listed in Table 2. According to Figs. 3 and 4, the FTIR spectra of quercetin and quercetin–Cu complexes show some of their characteristics, including:

1) The C=O stretching mode of the ligand quercetin occurred at 1 664 cm^{-1}, which disappeared due to the formation of the complexes. The coordination site for complex formation with Cu(II) may occur through the carbonyl atom and 3,5-OH groups of quercetin.

2) The bands at 1 560 (ν(C=C)) and 1 259 cm^{-1} (ν(C–O–C)) slightly shifted upon complexation.

3) The ν(C–O–H) deformation mode detected at 1 318 cm^{-1} in the standard quercetin shifted to 1 375 and 1 379 m^{-1} in the complexes, indicating a rise in the bond order. This change is typically seen when the ortho-phenolic ν(O–H) group on the quercetin B ring interacts with metals.

4) The occurrence of ν(Cu–O) stretching vibrations at 712 and 613 cm^{-1} in the spectra of metal complexes-i and -v, respectively, indicated the formation of a metal complex. In contrast, the ligand quercetin displayed no such bonds.

Table 2 Assignment of the prominent IR bands of quercetin–Cu(II) complexes in wavenumbers (cm^{-1})

Quercetin (cm^{-1})	Metal complex-i (cm^{-1})	Metal complex-v(cm^{-1})	Functional groups
3 260	3 232	3 241	ν (O–H)
1 664	—	—	ν (C=O)
1 609	1 604	1 604	ν ring (A and B)
1 560	1 564	1 564	ν (C=C)
—	1 517	1 509	ν ring C, ν C_4=O_2
—	1 406	1 441	*N* ring C, ν C_3–O_3
1 318	1 379	1 375	ν ring B, ν C_4–OH, ν C_3–OH
1 259	1 262	1 288	
—	712	613	ν (Cu–O)

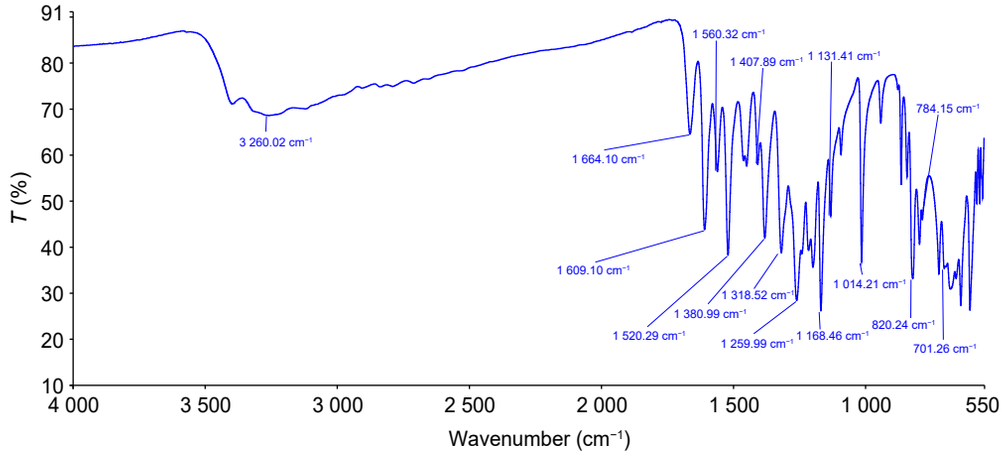

Fig. 3 The IR-spectra of quercetin.

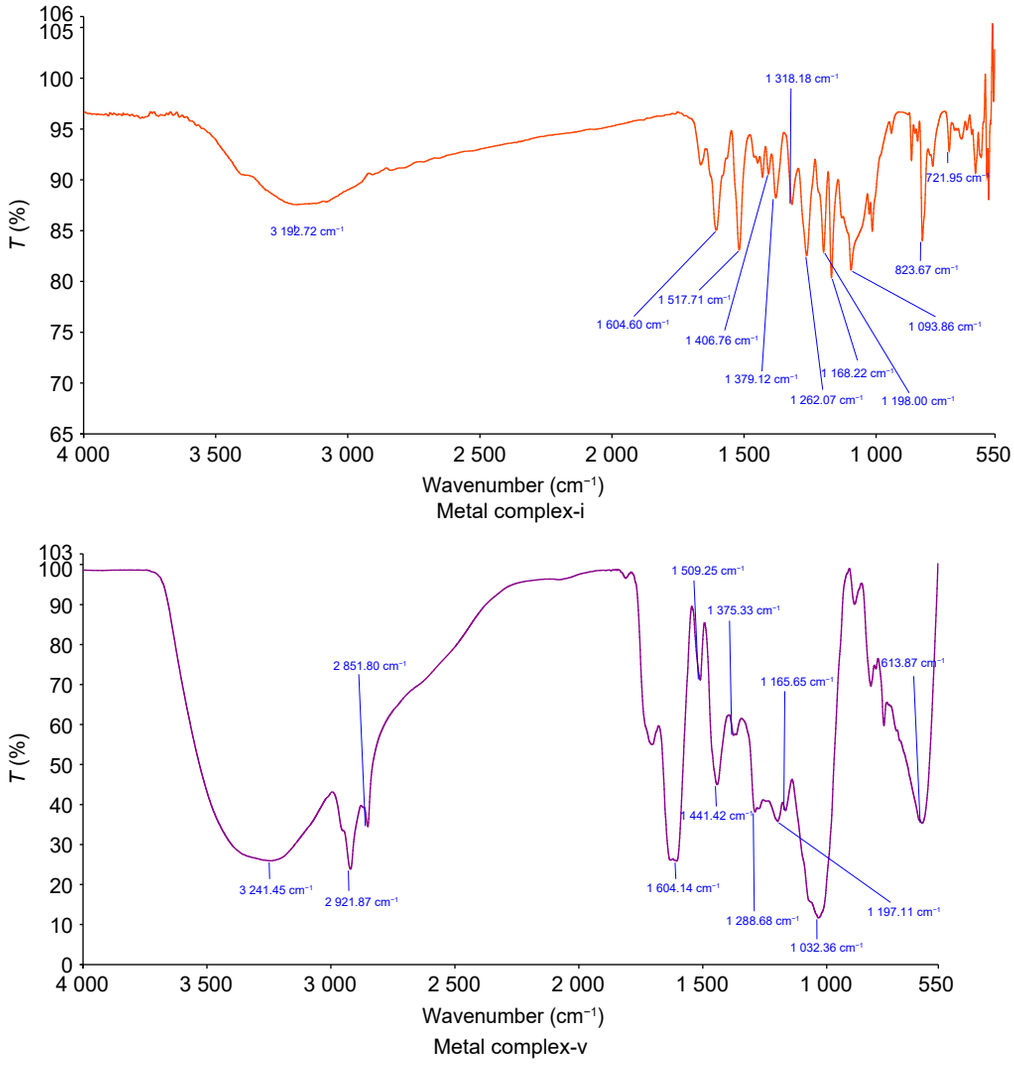

Fig. 4 The FTIR-spectra of metal complexes-i and -v.

5) *v*(O–H) frequencies appeared as extensive bands (3 690–2 390 cm^{-1}) and might be due to the presence of water, which can be verified by the thermal analysis of water.

Antioxidant activity

With metal complex-i (Quer–Cu) and metal complex-v(extracted Quer–Cu), the antioxidant activities were tested using the stable DPPH radical, reducing power, and linoleic acid assay.

DPPH assay

Figure 5 illustrates the antioxidant capacities of quercetin and quercetin–Cu(II) complexes. In general, the antioxidant capacities of quercetin–Cu(II) complexes were significantly higher than that of quercetin ($p<0.05$). At 100 g/mL, quercetin, standard quercetin–Cu complex (metal complex-i), and extracted quercetin–Cu complex (metal complex-v) had DPPH scavenging abilities of 63.25, 71.26, and 76.9%, respectively. The extracted quercetin–Cu(II) complex had the maximum capacity to scavenge free radicals when compared to the quercetin–Cu(II) complex as a whole.

Linoleic acid assay

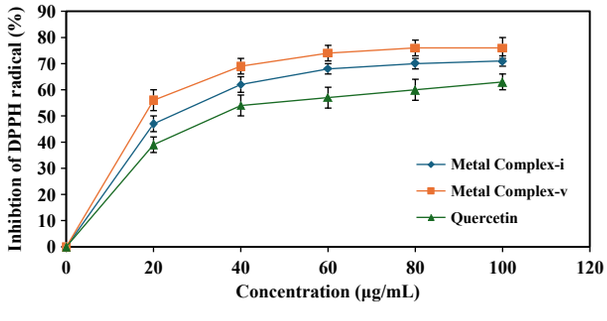

Fig. 5 The inhibition of DPPH radicals (%) by quercetin–Cu(II) complexes. The data are presented as the mean ± SD ($n = 3$; $p < 0.05$).

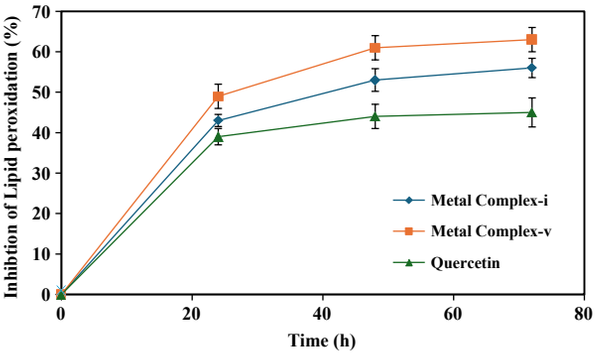

Fig. 6 The inhibition of lipid peroxidation. All data are reported as the mean ± SD (n = 3; p <0.05).

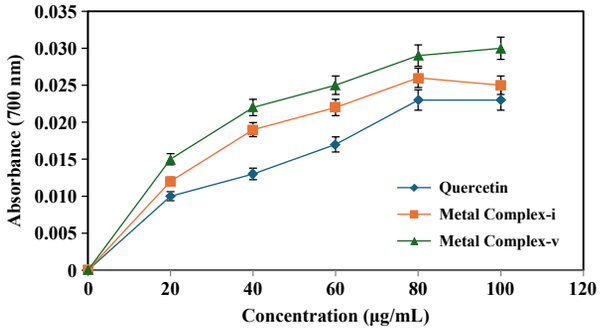

Fig. 7 Reducing power assay. All data are reported as the mean ± SD (n = 3; p < 0.05).

Figure 6 displays the suppression (%) of lipid peroxidation caused by quercetin and quercetin–Cu(II) complexes. In comparison to pure quercetin, quercetin–Cu(II) complexes demonstrated a considerable (p<0.05) decline in lipid peroxidation. At 72 h, the proportions of pure quercetin, quercetin–Cu complex (metal complex-i), and extracted quercetin–Cu complex (metal complex-v) that inhibited lipid peroxidation were 45.24%, 59.26%, and 63.2%. The antioxidant activity varied substantially depending on the date. Longer durations of incubation resulted in enhanced inhibition. The outcomes demonstrated that the extracted quercetin–Cu(II) complex had higher inhibition of lipid peroxidation in comparison to the typical quercetin–Cu(II) complex.

Measurement of the reducing power

The reducing powers are shown in Fig. 7. The quercetin–Cu(II) complexes showed a significant (p < 0.05) reducing power as compared to standard quercetin. Quercetin–Cu (metal complex-i) and extracted quercetin–Cu complexes (metal complex-v) had elevated reducing potential that was directly proportional to their concentration (20–100 µg/mL). In terms of reducing power, the extracted quercetin–Cu complex was the first (0.028), followed by the quercetin–Cu complex (0.025), and pure quercetin (0.023).

Anti-microbial activity

The anti-microbial activity of the synthesized quercetin–Cu(II) complexes has been assessed quantitatively by measuring the diameter of the inhibition zones (zones of no growth). The inhibition zone values of quercetin, metal complex-i, metal complex-v, and ciprofloxacin in *E. coli* are shown in Table 3. Metal complexes showed superior antimicrobial activity against *E. coli*. Limited activity was demonstrated by the minimum inhibitory concentration (20 mg/mL) against *E. coli*. Significantly (p < 0.05) vigorous activity was observed with 100 mg/mL of metal complex-v with an inhibition zone of (20 ± 1.00) mm in diameter, followed by metal complex-i at (19 ± 2.98) mm. However, the action of pure quercetin was minimal at (15 ± 1.00) mm. The antimicrobial activities of the synthesized metal complexes (standard and extracted) against *E. coli* were equivalent to those of standard antibiotics (zone of inhibition, 25 ± 2.78 mm). The quercetin–Cu complexes synthesized had higher anti-microbial activity than quercetin alone but lower than the standard ciprofloxacin.

The inhibition zone values of quercetin, metal

Table 3 Anti-microbial activity of quercetin and metal complexes against *Escherichia coli*

Compounds diameter of the bacterial inhibitory zone induced by ligand and complexes against *E. Coli* (Gram$^-$) (mm)					
	Concentrations				
	20 mg/mL	40 mg/mL	60 mg/mL	80 mg/mL	100 mg/mL
Metal complex-i	12 ± 1.04	14 ± 2.43	15.5 ± 2.11	16 ± 2.00	19 ± 2.98
Metal complex-v	13 ± 1.00	15 ± 2.41	16 ± 1.08	18 ± 2.09	20 ± 1.00
Quercetin	7 ± 0.056	10 ± 0.045	10 ± 0.052	12 ± 1.00	15 ± 1.00
Ciprofloxacin	15 ± 2.00	17 ± 1.06	20 ± 2.98	23 ± 2.67	25 ± 2.78

Note: All values of inhibition zones (mm) are presented as the mean ± SD (n = 3; p < 0.05).

Table 4 Anti-microbial activity of quercetin and metal complexes against *Bacillus subtilis*

Compounds diameter of bacterial inhibition zones induced by ligand and complexes against *B. subtilis* (Gram$^+$) (mm)					
	Concentrations				
	20 mg/mL	40 mg/mL	60 mg/mL	80 mg/mL	100 mg/mL
Metal complex-i	11 ± 1.03	12 ± 1.05	15 ± 1.00	18 ± 2.00	21 ± 2.54
Metal complex-v	11 ± 1.45	16 ± 1.00	19 ± 1.78	19 ± 1.78	23 ± 1.82
Quercetin	8 ± 1.00	8 ± 1.00	10 ± 0.03	13 ± 1.00	15 ± 2.00
Ciprofloxacin	15 ± 2.00	17 ± 1.67	22 ± 2.63	25 ± 2.53	27 ± 2.89

Note: All values of inhibition zones (mm) are presented as the mean ± SD ($n = 3$; $p < 0.05$).

complex-i, metal complex-v, and ciprofloxacin against *B. subtilis* are shown in Table 4. Metal complexes showed excellent activity against *B. subtilis* as compared to *E. coli*. The metal complex-v at 100 mg/mL strongly inhibited *B. subtilis* with an inhibition zone of (23 ± 1.82) mm, followed by metal complex-i (21 ± 2.54 mm) and pure quercetin (15 ± 2.00 mm). Inhibitory effects of the synthesized quercetin–Cu complexes (standard and extracted) against *B. subtilis* were comparable to those of the standard antibiotic (27 ± 2.89 mm). The quercetin–Cu complexes synthesized had biological activities that were greater than those of quercetin but lower than those of the standard ciprofloxacin.

Pharmacokinetic studies

Figure 8 depicts the mean plasma concentration–time curves for quercetin or quercetin–Cu complexes following oral administration with a single dose of 50 mg/kg. Figure 9 shows HPLC chromatograms of quercetin and extracted quercetin–Cu complexes in the plasma at time points of 0.5, 1, 2, 4, and 6 h. The most significant pharmacokinetic variables, including the maximum plasma concentration (C_{max}), the corresponding time (T_{max}), and the area under the plasma concentration-time curve (AUC), were provided in Table 5. As seen in Figure, plasma concentrations of the quercetin–Cu(II) complexes were consistently ($p < 0.05$) higher than those of pure quercetin at all-time points. The C_{max} value of quercetin–Cu(II) complexes (8.50 ± 0.26 mg/mL) at 1 h (T_{max}) was higher than that of pure quercetin (7.05 ± 0.33 mg/mL). After 24 h of oral administration of the quercetin–Cu(II) complex, its plasma concentration was higher (1.21 ± 0.53 mg/mL) than that of pure quercetin (0.76 ± 0.12 mg/mL). The AUC value of the quercetin–Cu(II) complex was 36.08 ± 1.07 mg/(h·mL), which was higher than that of standard quercetin (27.96 ± 0.32 mg/(h·mL)). The pharmacokinetic parameters indicated that the oral bioavailability of extracted quercetin–Cu(II) complexes was significantly enhanced as compared to standard quercetin.

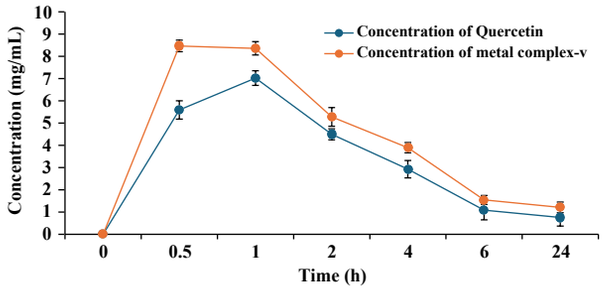

Fig. 8 The mean plasma concentration–time curves of quercetin or quercetin–Cu complexes in rats after a single dose of 50 mg/kg.

Conclusions

Because of quercetin's limited water solubility (0.17–7.7 g/mL), its use in medicine is severely constrained [48]. Therefore, new dosage forms of quercetin are urgently required, especially those with better solubility and greater bioavailability [49]. Quercetin-metal complexes improve the solubility and are ideal for the delivery of the active form [50, 51]. The colors of the complexes prepared with copper sulfate and copper chloride were dark yellow and brownish yellow, respectively [53, 54]. The change in the color of the solution indicated the formation of metal complexes. This result was further confirmed by UV–Vis spectroscopy, in which the benzoyl system (λ_1) of the complexes was similar, but the cinnamoyl system (λ_2) differed minutely. This finding suggested that the metal complex-v formation had taken place more significantly at band II. The shift in band II was due to the complexation of copper

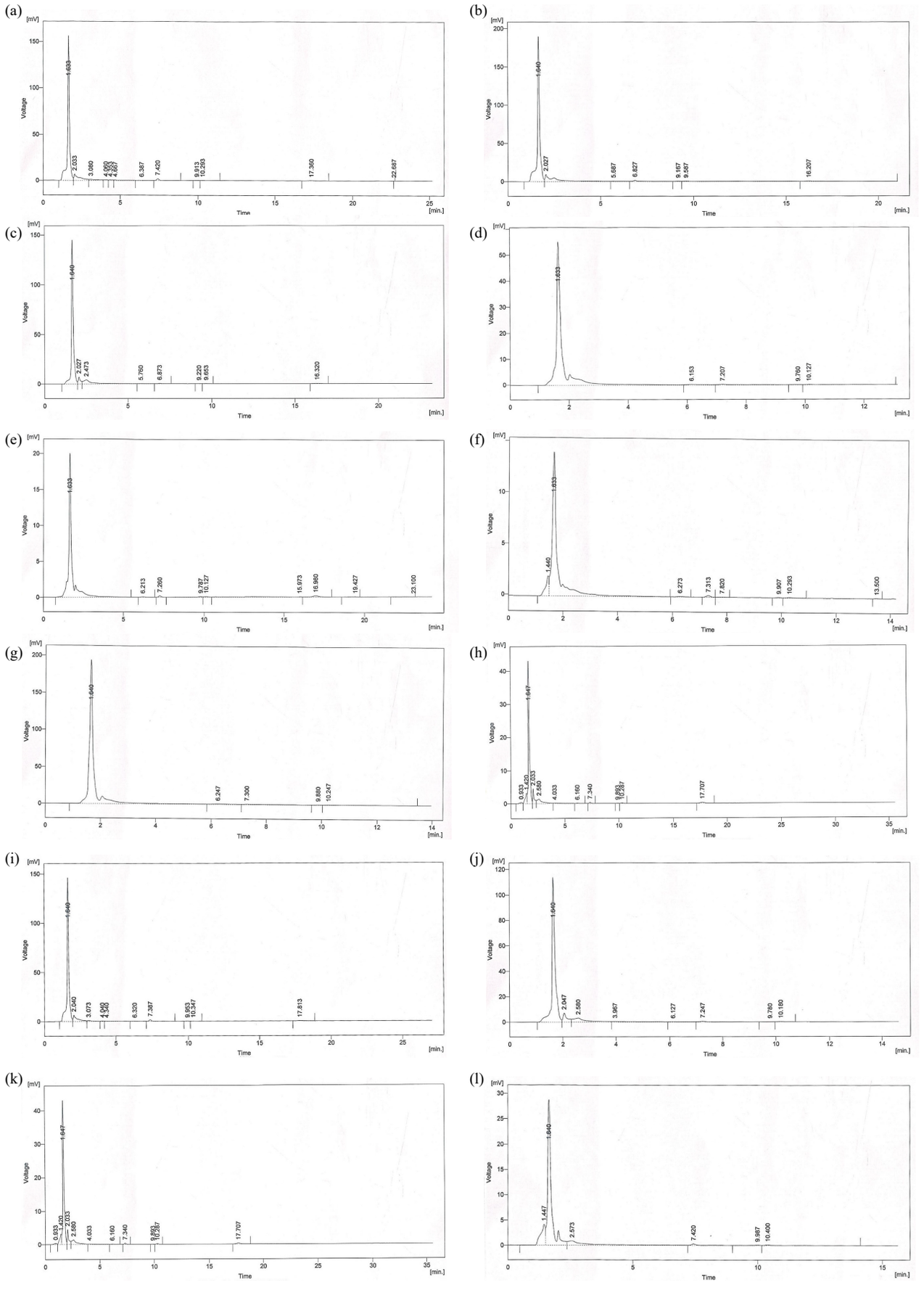

Fig. 9 High performance liquid chromatography (HPLC) chromatograms of the plasma levels of quercetin and metal complex-v. Quercetin at **(a)** 0.5 h, **(b)** 1 h, **(c)** 2 h, **(d)** 4 h, **(e)** 6 h, and **(f)** 24 h; metal complex-v at **(g)** 0.5 h, **(h)** 1 h, **(i)** 2 h, **(j)** 4 h, **(k)** 6 h, **(l)** 24 h.

Table 5 Pharmacokinetics parameters after oral administration of quercetin and quercetin–Cu complexes

Parameters	Quercetin	metal complex-v
T_{max}/h	1	0.5
C_{max}/(mg/mL)	7.056 21 ± 0.33	8.509 46 ± 0.26
AUC/(mg/h·mL)	27.961 ± 0.318 3	36.080 88 ± 1.071

at 3-OH and 4-C=O of quercetin [55]. The average experimental hypochromic shift in band II of Quer–Cu complexes was at 445 nm, which agreed with the value of 441 nm reported in the literature [56]. The average bathochromic shift in band I of the complexes was at 270 nm, which also coincided with the value of 269 nm reported in previous studies [57]. It can be concluded that the UV-Vis spectra from quercetin–Cu complexes (metal complex i, ii, iii, iv) and extracted quercetin-Cu complexes (metal complex v, vi, vii, viii) showed similar results (λ_1 = 269 nm, λ_2 = 441 nm). Thus, the standard and extracted quercetins had no marked impact on complex formation. Better quercetin–Cu complexes were observed at the ratio of 1:2 as compared to 1:1, the results between $CuSO_4$ and $CuCl_2$ were similar. The FTIR bands of ν (C=O) and ν (C=C) [ν ring C, ν C_4=O_2, ν ring C, ν C_3–O_3] disappeared, indicating complex formation [58]. A new characteristic band of ν (Cu–O) appeared at 613 cm^{-1} which matched with the reported value of 603 cm^{-1} [59], while the ligand quercetin showed no such band. The FTIR bands of standard quercetin–Cu complexes and extracted quercetin–Cu complexes were nearly similar. Thus, the extracted quercetin could be used for the metal complex preparation. DPPH scavenging activity by quercetin-metal complexes has been extensively reported. But the information regarding the reducing potential of quercetin–Cu(II) complexes and the inhibition of lipid peroxidation is limited. The findings of this study demonstrate the significant potential of the extracted quercetin–Cu(II) complexes (metal complex-v) in all antioxidant assays. They significantly impacted the DPPH scavenging assay, inhibited the lipid peroxidation assay, and had a lesser marked influence on the reducing power assay. The presence of various types of flavonoids in the extracted quercitin–Cu complexes may contribute to their antioxidant abilities. Hence, they could be used as the potential pharmaceuticals. In addition,the pharmacokinetic studies demonstrated the extracted quercetin–Cu(II) complexes could be the good choice of delivering antibiotics. The outcomes of this study also agreed with past reports which suggested that *B. subtilis* was more sensitive to metal complexes than *E. coli*. Our findings also concurred with the improved oral bioavailability of quercetin in the form of metal complexes reported recently [60–67].

CRediT Author Statement

Faiq Saeed and **Samia Arain** conceived the project, designed the experiments, intercepted the data, and finalized the manuscript. The first draft of the manuscript was written by **Sidra Javed**, **Nazish Jahan**, and **Zillie Huma**. **Muhammad Ishaq Ali**, **Amir Zada**, and **Aliya Ibrar** performed all the chemical measurements and recorded the data. **Ghulam Abbas Ashraf**, **Laila Noureen**, and **Muhammad Ayaz** provided material and helped in Graphs and images. All authors revised and commented on the manuscript.

Acknowledgements

We acknowledge the support from National Natural Science Foundation of China (No. 22274109). We are grateful to Tianjin Key Laboratory of Molecular Optoelectronic Science, Department of Chemistry, School of Science, Tianjin University for providing facility to carry out a part of the research.

Conflict of Interests

The authors declare no conflict of interest.

References

[1] P. Karak. Biological activities of flavonoids: an overview. *International Journal of Pharmaceutical Sciences and Research*, 2019, 10(4): 1567−1574. https://doi.org/10.13040/IJPSR.0975-8232.10(4).1567-74

[2] A. González-Sarrías, F.A. Tomás-Barberán, R. García-Villalba. Structural diversity of polyphenols and distribution in foods. In: Dietary Polyphenols: Their Metabolism and Health Effects, 2020: 1–29. https://doi.org/10.1002/9781119563754.ch1

[3] A.K. Anal. Quality ingredients and safety concerns for traditional fermented foods and beverages from Asia: A review. *Fermentation*, 2019, 5(1): 8. https://doi.org/10.3390/fermentation5010008

[4] M. Symonowicz, M. Kolanek. Flavonoids and their properties to form chelate complexes. *Biotechnology and*

Food Sciences, 2012, 76(1): 35−41.
[5] S. Mondal, T.R. Syed. Flavonoids: A vital resource in healthcare and medicine. *Pharmacy & Pharmacology International Journal*, 2020, 8(2): 91−104. https://doi.org/10.15406/ppij.2020.08.00285
[6] N. Bordenave, B.R. Hamaker, M.G. Ferruzzi. Nature and consequences of non-covalent interactions between flavonoids and macronutrients in foods. *Food & Function*, 2014, 5(1): 18−34. https://doi.org/10.1039/C3FO60263J
[7] B.H. Havsteen. The biochemistry and medical significance of the flavonoids. *Pharmacology & Therapeutics*, 2002, 96(2-3): 67−202. https://doi.org/10.1016/s0163-7258(02)00298-x
[8] D.O. Kim, C.Y. Lee. Comprehensive study on vitamin C equivalent antioxidant capacity (VCEAC) of various polyphenolics in scavenging a free radical and its structural relationship. *Critical Reviews in Food Science and Nutrition*, 2004, 44(4): 253−273. https://doi.org/10.1080/10408690490464960
[9] A. Barman, C.M. Marak, R. Mitra Barman, et al. Nutraceutical properties of legume seeds and their impact on human health. In: Legume Seed Nutraceutical Research. IntechOpen, 2019. https://doi.org/10.5772/intechopen.78799
[10] G.W. Canonica, M. Blaiss. Antihistaminic, anti-inflammatory, and antiallergic properties of the nonsedating second-generation antihistamine desloratadine: A review of the evidence. *World Allergy Organization Journal*, 2011, 4(2): 47−53. https://doi.org/10.1097/WOX.0b013e3182093e1
[11] N.P. Seeram, M.G. Nair. Inhibition of lipid peroxidation and structure-activity-related studies of the dietary constituents anthocyanins, anthocyanidins, and catechins. *Journal of Agricultural and Food Chemistry*, 2002, 50(19): 5308−5312. https://doi.org/10.1021/jf025671q
[12] R.V. Patel, B.M. Mistry, S.K. Shinde, et al. Therapeutic potential of quercetin as a cardiovascular agent. *European Journal of Medicinal Chemistry*, 2018, 155: 889−904. https://doi.org/10.1016/j.ejmech.2018.06.053
[13] G. El-Saber Batiha, A.M. Beshbishy, M. Ikram, et al. The pharmacological activity, biochemical properties, and pharmacokinetics of the major natural polyphenolic flavonoid: quercetin. *Foods*, 2020, 9(3): 374. https://doi.org/10.3390/foods9030374
[14] Y. Wang, B.X. Tao, Y. Wan, et al. Drug delivery based pharmacological enhancement and current insights of quercetin with therapeutic potential against oral diseases. *Biomedicine & Pharmacotherapy = Biomedecine & Pharmacotherapie*, 2020, 128: 110372. https://linkinghub.elsevier.com/retrieve/pii/S0753332220305655
[15] J.S. Mu, X. Zhao, J. Li, et al. Novel hierarchical NiO nanoflowers exhibiting intrinsic superoxide dismutase-like activity. *Journal of Materials Chemistry B*, 2016, 4(31): 5217−5221. https://doi.org/10.1039/C6TB01390B
[16] H. Wake, Y. Takahashi, Y. Yoshii, et al. Histidine-rich glycoprotein possesses antioxidant activity through self-oxidation and inhibition of hydroxyl radical production via chelating divalent metal ions in Fenton's reaction. *Free Radical Research*, 2020, 54(8-9): 649−661. https://doi.org/10.1080/10715762.2020.1825703
[17] H.G. Ulusoy, N. Sanlier. A minireview of quercetin: From its metabolism to possible mechanisms of its biological activities. *Critical Reviews in Food Science and Nutrition*, 2020, 60(19): 3290−3303. https://doi.org/10.1080/10408398.2019.1683810
[18] L.W. Zhang, Z.B. Shang, K.X. Guo, et al. Speciation analysis and speciation transformation of heavy metal ions in passivation process with thiol-functionalized nano-silica. *Chemical Engineering Journal*, 2019, 369: 979−987. https://doi.org/10.1016/j.cej.2019.03.077
[19] M. Hofmann, G. Retamal-Morales, D. Tischler. Metal binding ability of microbial natural metal chelators and potential applications. *Natural Product Reports*, 2020, 37(9): 1262−1283. https://doi.org/10.1039/C9NP00058E
[20] M. Zhang, S.W. Cui, P.C.K. Cheung, et al. Antitumor polysaccharides from mushrooms: A review on their isolation process, structural characteristics and antitumor activity. *Trends in Food Science and Technology*, 2007, 18(1): 4−19. https://doi.org/10.1016/j.tifs.2006.07.013
[21] D.J.S.N. Strain. Body & brain: Allergies might fights off cancer: Elevated immune response could target some tumors. 2011. 179(6): 12. [INVALID]
[22] A. Czerwonka, U. Maciołek, J. Kałafut, et al. Anticancer effects of sodium and potassium quercetin-5'-sulfonates through inhibition of proliferation, induction of apoptosis, and cell cycle arrest in the HT-29 human adenocarcinoma cell line. *Bioorganic Chemistry*, 2020, 94: 103426. https://doi.org/10.1016/j.bioorg.2019.103426
[23] P. Sharma, T. Joshi, T. Joshi, et al. In silico screening of potential antidiabetic phytochemicals from Phyllanthus emblica against therapeutic targets of type 2 diabetes. *Journal of Ethnopharmacology*, 2020, 248: 112268. https://doi.org/10.1016/j.jep.2019.112268
[24] S. Nangare, S. Patil, K. Chaudhari, et al. Graphene quantum dots incorporated UiO-66-NH2 based fluorescent nanocomposite for highly sensitive detection of quercetin. *Nano Biomedicine and Engineering*, 2023, 15(1): 1−13. https://doi.org/10.26599/NBE.2023.9290005
[25] F. Damiano, L. Giannotti, G.V. Gnoni, et al. Quercetin inhibition of SREBPs and ChREBP expression results in reduced cholesterol and fatty acid synthesis in C6 glioma cells. *The International Journal of Biochemistry & Cell Biology*, 2019, 117: 105618. https://doi.org/10.1016/j.biocel.2019.105618
[26] J.N. Okolle. Research notes on current issues in cameroon agriculture. *Forum for Agricultural Research in Africa*, 2019, 4(14): 169.
[27] T.N. Ravishankar, K. Manjunatha, T. Ramakrishnappa, et al. Comparison of the photocatalytic degradation of trypan blue by undoped and silver-doped zinc oxide nanoparticles. *Materials Science in Semiconductor Processing*, 2014, 26: 7−17. https://doi.org/10.1016/j.mssp.2014.03.027
[28] M. Nawaz, G. Camussi, H. Valadi, et al. The emerging role of extracellular vesicles as biomarkers for urogenital cancers. *Nature Reviews Urology*, 2014, 11(12): 688−701. https://doi.org/10.1038/nrurol.2014.301
[29] L. Forte, P. Torricelli, E. Boanini, et al. Quercetin and alendronate multi-functionalized materials as tools to hinder oxidative stress damage. *Journal of Biomedical Materials Research Part A*, 2017, 105(12): 3293−3303. https://doi.org/10.1002/jbm.a.36192
[30] A. Pękal, M. Biesaga, K. Pyrzynska. Interaction of quercetin with copper ions: Complexation, oxidation and reactivity towards radicals. *BioMetals*, 2011, 24(1): 41−49. https://doi.org/10.1007/s10534-010-9372-7
[31] S.B. Bukhari, S. Memon, M. Mahroof-Tahir, et al. Synthesis, characterization and antioxidant activity copper–quercetin complex. *Spectrochimica Acta Part A: Molecular and Biomolecular Spectroscopy*, 2009, 71(5): 1901−1906. https://doi.org/10.1016/j.saa.2008.07.030
[32] H.F. Talab, I.A. Zabani, H.S. Abdelrahman, et al. Intraoperative ventilatory strategies for prevention of pulmonary atelectasis in obese patients undergoing laparoscopic bariatric surgery. *Anesthesia and Analgesia*,

2009, 109(5): 1511−1516. https://doi.org/10.1213/ANE.0b013e3181ba7945

[33] H. Lewandowska, M. Kalinowska, W. Lewandowski, et al. The role of natural polyphenols in cell signaling and cytoprotection against cancer development. *The Journal of Nutritional Biochemistry*, 2016, 32: 1−19. https://doi.org/10.1016/j.jnutbio.2015.11.006

[34] B.H. Chang, S.H. Lee, A. Lyengar, et al. Chemical grafting of new poly (aminophenyl bornoic acid) chains onto the surface of silica nanoparticles. *Advanced Materials Research*, 2013, 717: 90−94. https://doi.org/10.4028/www.scientific.net/AMR.717.90

[35] S.R. Palle, J. Penchalaneni, K. Lavudi, et al. Green synthesis of silver nanoparticles by leaf extracts of boerhavia erecta and spectral characterization and their antimicrobial, antioxidant ad cytotoxic studies on ovarian cancer cell lines. *Letters in Applied NanoScience*, 2020, 9(3): 1165−1176. https://doi.org/10.33263/LIANBS93.11651176

[36] Vansyngel, F., et al., Statistical simulations of the dust foreground to cosmic microwave background polarization. 2017. 603: p. A62.

[37] F. Vansyngel, F. Boulanger, T. Ghosh, et al. Statistical simulations of the dust foreground to cosmic microwave background polarization. *Astronomy & Astrophysics*, 2017, 603: A62. https://doi.org/10.1051/0004-6361/201629992

[38] H. Bellia, R. Youcef, M. Fatima. A detailed modeling of photovoltaic module using MATLAB. *NRIAG Journal of Astronomy and Geophysics*, 2014, 3(1): 53−61. https://doi.org/10.1016/j.nrjag.2014.04.001

[39] L. Barros, M.J. Ferreira, B. Queirós, et al. Total phenols, ascorbic acid, β-carotene and lycopene in Portuguese wild edible mushrooms and their antioxidant activities. *Food Chemistry*, 2007, 103(2): 413−419. https://doi.org/10.1016/j.foodchem.2006.07.038

[40] R. Ronen, M. Galun,. Pigment extraction from lichens with dimethyl sulfoxide (DMSO) and estimation of chlorophyll degradation. *Environmental and Experimental Botany*, 1984, 24(3): 239−245. https://doi.org/10.1016/0098-8472(84)90004-2

[41] G. Deepa, S. Ayesha, K. Nishtha, et al. Comparative evaluation of various total antioxidant capacity assays applied to phytochemical compounds of Indian culinary spices. *International Food Research Journal*, 2013, 20(4): 1711−1716.

[42] S. Fourati, R. Cristescu, A. Loboda, et al. Pre-vaccination inflammation and B-cell signalling predict age-related hyporesponse to hepatitis B vaccination. *Nature Communications*, 2016, 7: 10369. https://doi.org/10.1038/ncomms10369

[43] S. Fujisaka, I. Usui, A. Bukhari, et al. Regulatory mechanisms for adipose tissue M1 and M2 macrophages in diet-induced obese mice. *Diabetes*, 2009, 58(11): 2574−2582. https://doi.org/10.2337/db08-1475

[44] D.S. Raie, E. Mhatre, M.nThiele, et al. Application of quercetin and its bio-inspired nanoparticles as anti-adhesive agents against Bacillus subtilis attachment to surface. *Materials Science and Engineering: C*, 2017, 70(pt 1): 753–762. https://doi.org/10.1016/j.msec.2016.09.038

[45] M. Stone, D. Brambilla, K. Murcia, et al. Feasibility of routine ferritin testing for donor management: Validation of delayed processing and demonstration of within donor reproducibility over time. *Transfusion*, 2016, 56(10): 2422−2425. https://doi.org/10.1111/trf.13793

[46] T. Kawasaki, T. Iwasaki, I. Ohya, et al. Effects of sampling and storage method on chicken blood glucose measurement. *The Journal of Poultry Science*, 2020, 57(3): 241−245. https://doi.org/10.2141/jpsa.0190106

[47] G.H. Guo, J. Dong, X.H. Yuan, et al. Clinical evaluation of the levels of 12 cytokines in serum/plasma under various storage conditions using evidence biochip arrays. *Molecular Medicine Reports*, 2013, 7(3): 775−780. https://doi.org/10.3892/mmr.2013.1263

[48] H. Wu, S.Y. Sun, K. Tu, et al. A splicing-independent function of SF_2/ASF in microRNA processing. *Molecular Cell*, 2010, 38(1): 67−77. https://doi.org/10.1016/j.molcel.2010.02.021

[49] J.-C. Zhang, S.-X. Li, K. Hashimoto. R(–)-ketamine shows greater potency and longer lasting antidepressant effects than S (+)-ketamine. *Pharmacology Biochemistry and Behavior*, 2014, 116: 137−141. https://doi.org/10.1016/j.pbb.2013.11.033

[50] P. Mukhopadhyay, S. Maity, S. Mandal, et al. Preparation, characterization and *in vivo* evaluation of pH sensitive, safe quercetin-succinylated chitosan-alginate core-shell-corona nanoparticle for diabetes treatment. *Carbohydrate Polymers*, 2018, 182: 42−51. https://doi.org/10.1016/j.carbpol.2017.10.098

[51] A.A. Date, M.S. Nagarsenker, S. Patere, et al. Lecithin-based novel cationic nanocarriers (leciplex) II: Improving therapeutic efficacy of quercetin on oral administration. *Molecular Pharmaceutics*, 2011, 8(3): 716−726. https://doi.org/10.1021/mp100305h

[52] P. Sathishkumar, Z.F. Li, R. Govindan, et al. Zinc oxide-quercetin nanocomposite as a smart nano-drug delivery system: Molecular-level interaction studies. *Applied Surface Science*, 2021, 536: 147741. https://doi.org/10.1016/j.apsusc.2020.147741

[53] L. Xiao, G. Luo, Y.H. Tang, et al. Quercetin and iron metabolism: What we know and what we need to know. *Food and Chemical Toxicology*, 2018, 114: 190−203. https://doi.org/10.1016/j.fct.2018.02.022

[54] T. Muthurajan, P. Rammanohar, N.P. Rajemdran, et al. Evaluation of a quercetin–gadolinium complex as an efficient positive contrast enhancer for magnetic resonance imaging. *RSC Advances*, 2015, 5(106): 86967−86979. https://doi.org/10.1039/C5RA16405B

[55] D.M. Lebensztejn, M. Flisiak-Jackiewicz, I. Białokoz-Kalinowska, et al. Hepatokines and non-alcoholic fatty liver disease. *Acta Biochimica Polonica*, 2016, 63(3): 459−467. https://doi.org/10.18388/abp.2016_1252

[56] E.M.M. Abdelraheem, K. Kurpiewska, J. Kalinowska-Tłuścik, et al. Artificial macrocycles by ugi reaction and passerini ring closure. *The Journal of Organic Chemistry*, 2016, 81(19): 8789−8795. https://doi.org/10.1021/acs.joc.6b01430

[57] S.S. Hasan, S.I. Ahmed, N.I. Bukhari, et al. Use of complementary and alternative medicine among patients with chronic diseases at outpatient clinics. *Complementary Therapies in Clinical Practice*, 2009, 15(3): 152−157. https://doi.org/10.1016/j.ctcp.2009.02.003

[58] S. Balsam, G.D. Fernando, A. Tripathy. The impact of firm strategy on performance measures used in executive compensation. *Journal of Business Research*, 2011, 64(2): 187−193. https://doi.org/10.1016/j.jbusres.2010.01.006

[59] S.S. Bukhari, F. Shafait, T.M. Breuel. Script-independent handwritten textlines segmentation using active contours. In: 2009 10th International Conference on Document Analysis and Recognition, 2009. https://doi.org/10.1109/icdar.2009.206 https://doi.org/10.1109/icdar.2009.206

[60] P. Ghosh, B. Rathinasabapathi, L.Q. Ma. Phosphorus

solubilization and plant growth enhancement by arsenic-resistant bacteria. *Chemosphere*, 2015, 134: 1−6. https://doi.org/10.1016/j.chemosphere.2015.03.048

[61] X. Yang, R. Kwitt, M. Styner, et al. Quicksilver: Fast predictive image registration–A deep learning approach. *NeuroImage*, 2017, 158: 378−396. https://doi.org/10.1016/j.neuroimage.2017.07.008

[62] H.M. Tauqeer, S. Ali, M. Rizwan, et al. Phytoremediation of heavy metals by Alternanthera bettzickiana: Growth and physiological response. *Ecotoxicology and Environmental Safety*, 2016, 126: 138−146. https://doi.org/10.1016/j.ecoenv.2015.12.031

[63] F. Saeed, M. Ahmad, Samia, et al. Phosphorus-doped $CoFe_2O_4$ nanoparticles decorated nitrogen-doped graphene for efficient and stable electrocatalytic water splitting. *International Journal of Hydrogen Energy*, 2024, 59: 1196−1204. https://doi.org/10.1016/j.ijhydene.2024.01.035

[64] Samia, F. Saeed, J. Li, et al. Emerging trends in metal-organic framework (MOFs) photocatalysts for hydrogen energy using water splitting: A state-of-the-art review. *Journal of Industrial and Engineering Chemistry*, 2024, 131: 54−135. https://doi.org/10.1016/j.jiec.2023.10.055

[65] G.A. Ashraf, R.T. Rasool, M.M. Fadhali, et al. Novel magnetic Carbon@$BaBiFe_{12}O_{19}$ photocatalyst for efficient pollutants degradation under peroxymonosulfate activation. *Materials Science in Semiconductor Processing*, 2024, 176: 108291. https://doi.org/10.1016/j.mssp.2024.108291

[66] A. Ibrar, S.A. Shehzadi, F. Saeed, et al. Developing hybrid molecule therapeutics for diverse enzyme inhibitory action: Active role of coumarin-based structural leads in drug discovery. *Bioorganic & Medicinal Chemistry*, 2018, 26(13): 3731−3762. https://doi.org/10.1016/j.bmc.2018.05.042

[67] R. Amin, B.S. Liu, S. Ullah, et al. Study of mass transfer resistant effect during syn gas and hydrogen production through CO_2/CH_4 dry reforming on La/Mg supported co-Ni/MSU-S zeolite. *The Lighthouse Journal of Natural Sciences*, 2022, 1(02): 19−34.